Pergamon

PII: S0042-6989(96)00327-6

Vision Res., Vol. 37, No. 13, pp. 1829–1844, 1997
© 1997 Elsevier Science Ltd. All rights reserved
Printed in Great Britain
0042-6989/97 $17.00 + 0.00

Implementations of a Novel Algorithm for Colour Constancy

F. MARTÍNEZ-VERDÚ,*† M. J. LUQUE,* J. MALO,* A. FELIPE,* J. M. ARTIGAS*

Received 6 April 1995; in revised form 2 August 1996; in final form 8 November 1996

In agreement with the principles of the relativistic model proposed by Creutzfeldt *et al.*, with the photometric rule (lightness anchoring rule) and with the influence of simultaneous contrast in the appearance of a visual scene, we propose a first-stage mechanism yielding substantial colour constancy. We have defined a set of first-stage colour descriptors, and to test their utility, we have performed a simulation using a Machine Vision System (MVS). The statistical stability of the descriptors for Munsell samples under different illuminants is good. © 1997 Elsevier Science Ltd.

Colour constancy | Photometric rule | Simultaneous contrast | Chromatic adaptation | Computer simulation

INTRODUCTION

The colour constancy property of the human visual system (HVS) is the perceptual capability to assign approximately the same chromatic attributes—brightness, hue and chroma—to stimuli that differ colorimetrically due to a spectral change in the illuminant. It seems, therefore, that the visual system is able to construct a perceptual invariant from the information conveyed in colour signals. The experiments of E. H. Land (1977, 1986) and R. W. G. Hunt (1979, 1991) are typical psychophysical demonstrations of this capability.

It is commonly accepted that the visual system (low-level mechanisms of chromatic adaptation) can perform an adaptive shift in the initial chromatic description of a given stimulus that maintains approximately the same colour appearance under physical shifts in the stimulus energy that occur as a consequence of spectral changes in the illuminant (Wyszecki, 1986). Nevertheless, many psychophysical experiments show that these adaptive shifts are not completely effective in maintaining constant colour appearance. Many studies have found small systematic deviations from constancy in the perception of chromatic attributes under the illuminant changes (Worthey, 1985; Arend & Reeves, 1986; Blackwell & Buchsbaum, 1988; Valberg & Lange-Malecki, 1990; Arend *et al.*, 1991; Arend, 1993).

Other phenomena that influence or limit colour constancy are metamerism and simultaneous contrast. Metamers are lights of different spectral composition that evoke the same visual response. Metamerism is an inescapable result of the principle of univariance in the chromatic encoding performed by the long-(L), medium-(M) and short-(S) wavelength photoreceptors. The perceptual phenomenon of simultaneous contrast or chromatic induction, on the other hand, gives evidence of one mechanism by which the visual system may compute constant chromatic attributes in continually changing environments. It might even be said that simultaneous contrast causes colour constancy (Hunt, 1979, 1991); but one might also ask whether colour constancy causes chromatic induction (Walraven *et al.*, 1987).

It is generally accepted that simultaneous contrast is the cornerstone of colour constancy in those colour constancy results from comparisons between surface colours within a scene. Indeed, some definitions of colour constancy include invariance within the set of coloured areas in the scene (Craven & Foster, 1992). Further, some experiments show the special relevance of chromatic induction (Krauskopf *et al.*, 1986; Valberg & Lange-Malecki, 1990; Cornelissen & Brenner, 1995; Luo *et al.*, 1995; Jin & Shevell, 1996). The work of Arend and co-workers (Arend & Reeves, 1986; Arend *et al.*, 1991) suggests that the visual system can use spatially and chromatically related colour stimuli—i.e., those of similar hue—in a scene to perform asymmetrical matches to keep a colour stimulus constant under changes in the illuminant (*paper match*). The works of Baüml (1994, 1995) attest that the gamut of colour stimuli in the scene is also a major influence on the subjective matching of an supposedly achromatic stimulus.

Without colour constancy, Machine Vision Systems (MVS) detect only the colorimetric shifts of surfaces

*Dpto. de Óptica. Facultad de Física. Universitat de València. C/ Dr. Moliner, 50. 46100-Burjassot, València, Spain.

†To whom all correspondence should be addressed at present address: Dpt. d'Òptica i Optometria de la Escola Universitària d'Òptica i Optometria de Terrassa (EUOOT), Universitat Politècnica de Catalunya, C/ Violinista Vellsolà, 37. 08222-Terrassa, Barcelona, Spain [*Email* fmartinez@oo.upc.es].

under illuminant shifts. If we wish to implement illuminant-invariant chromatic encoding algorithms on these devices, it would be very helpful to understand underlying colour constancy mechanisms as achieved by the Human Vision System (HVS) (Webster & Mollon, 1993; Maloney, 1994; Singer & D'Zmura, 1995).

The current theories of colour constancy can be classified into three groups as follows: (1) first stage algorithmic models, with non-linear chromatic contrast, that use the white stimulus as a reference (von Kries, 1905; Hurlbert, 1986; Land, 1986; Worthey & Brill, 1986; Lucassen & Walraven, 1993, 1996); (2) second stage algorithmic models that retain some colorimetric character and postulate a second processing of the output signal of the first-stage mechanisms (by means of an opponent formalism [for instance Nayatani *et al.* (1987) and Hunt (1991)]; and (3) linear models for surface spectral reflectance reconstruction, based on some restrictions on the representation spaces of the reflectances and the illuminants, on the dimensional character of colour encoding (dichromacy, trichromacy, tetrachromacy, etc.), on the number of colour stimuli in the scene, and on the number of possible viewings of the scene under different illuminants (Maloney & Wandell, 1986; D'Zmura & Iverson, 1994). At present, there are some new strategies that combine some points of the previous models; in particular, diagonal matrix transform approaches (Brill, 1993; Finlayson *et al.*, 1994) and colour histogram image transform approaches (Healey & Slater, 1994; Funt & Finlayson, 1995; Martínez-Verdú *et al.*, 1996).

In this paper, we have made use of the relativistic model of chromatic induction by Creutzfeldt *et al.* (1990), of the photometric rule or lightness anchoring rule—the familiar highest-luminance-as-white rule—(Bonato *et al.*, 1992; Li & Gilchrist, 1993) and of some characteristics of simultaneous contrast related to chromatic adaptation, to design a set of first-stage colour descriptors (α_{ij}, β_{ij}, γ_{ij}) for any colour stimulus in the scene, independently of the presence or absence of a white stimulus. This encoding incorporates lateral inhibition between photoreceptors of the same type, which accounts for simultaneous contrast phenomena, and it is scaled by the response range within each photoreceptor type, which yield contrast adaptation. As an application of the functionality of this first-stage mechanism through (α_{ij}, β_{ij}, γ_{ij}) we have focused our work on problems related to colour constancy. We have computed the descriptors for different types of lateral inhibition represented by subtracting different references. From this viewpoint we have distinguished between "achromatic" relativistic spaces—which refer to a white ($\alpha_{i\mathrm{W}}$, $\beta_{i\mathrm{W}}$, $\gamma_{i\mathrm{W}}$) or a black ($\alpha_{i\mathrm{BK}}$, $\beta_{i\mathrm{BK}}$, $\gamma_{i\mathrm{BK}}$) stimulus—and "chromatic" relativistic spaces, which refer to hues. Though we do not discard the possible improvements on colour constancy of a second-stage mechanism (opponent processing), we have tested the goodness of these first-stage descriptors when implemented in a typical machine vision system. Finally, we have found our results to be consistent with those of related works, in particular with those of Arend and co-workers.

THEORETICAL BASIS AND METHOD

A complete colour constancy algorithm that describes the behaviour of the human visual system or that is to be implemented on a machine vision system, must clearly distinguish between a first stage of chromatic contrast processing and a second one of construction in a perceptual space. Thus, Land, with the elaboration of his Retinex theory, might have meant by the name "retinex" that the initial stage occurred probably at the retinal level, whereas the computation of perceptual variables brightness, hue and chroma presumably occurred at cortical levels.

Still, the Retinex theory is just a first-stage colour constancy algorithm. That is, it assumes that the visual system encodes each colour stimulus according to its lightness in the L, M and S channels. In the original Retinex, lightness is computed from the chromatic contrast in the borders between colour stimuli using a white (W) stimulus as a reference. In a sense, this approach to the problem is consistent with the interactive colour contrast mechanisms proposed in the 19th century (Fechner, 1890; Mach, 1866), and more explicitly during the last decades (Hurvich & Jameson, 1964; Land & McCann, 1971). The objective of all these models and mechanisms is to clarify the role that simultaneous contrast phenomena play in the way the human visual system encodes colour in general, and in colour constancy in particular.

Recently, O. Creutzfeldt and co-workers (Creutzfeldt *et al.*, 1990) performed a series of experiments using a center–surround paradigm showing that lateral inhibition between photoreceptors of the same channel might explain, simply and qualitatively, many chromatic induction phenomena. Their results show that the visual system does not add directly the response strengths of the different spectral components of a colour stimulus; rather, the signals are scaled according to their brightnesses in each spectral domain defined, e.g., by cone spectral sensitivities or colour matching functions. These conclusions are consistent with von Kries-type models (von Kries, 1905; Wyszecki & Stiles, 1982; Land, 1986; Lucassen *et al.*, 1993, 1996). Furthermore, chromaticity (i.e., hue and chroma) and brightness are not independent at this stage, which is consistent with neurophysiological evidence (Creutzfeldt *et al.*, 1983; Valberg *et al.*, 1987).

In this relativistic colour model for chromatic induction, it was assumed that, at a first stage, the brightness of the stimulus was determined in each spectral domain by means of a comparison between the strengths of the object and the surround. This information is supplied by the spatial arrangement of the receptive fields of the retina sensorial units. This scaled brightness value is then the input signal for the opponent channels (second stage), whose outputs are combined to give the perceived colour. This is consistent with neurophysiological evidence indicating that brightness evaluation is carried out early

in the visual process. The signals proposed were a linear subtraction of the intensities of center and surround, as suggested by experiments on brightness measurement (Hurvich & Jameson, 1964; Takasaki, 1969; Walraven, 1976; Creutzfeldt *et al.*, 1987; Valberg *et al.*, 1987).

In this work, we propose a first-stage process in which we describe the relative scaling of brightness in the different spectral domains and the lateral inhibition of the photoreceptors. This process is analytically expressed by means of the first-stage colour descriptors (α_{ij}, β_{ij}, γ_{ij}), calculated as follows:

$$\alpha_{ij} = \frac{\log(R_i + 1) - \log(R_j + 1)}{\log(R_{\max} - R_{\min} + 1)} \times 100 \qquad (1)$$

where:

i,j: colour stimuli from a set of n stimuli present in the scene;

R_i: receptoral capture or strength (intensity) of stimulus i in the k spectral domain or channel (R or L, G or M, B or S).

In a more general way, R_i, or, equivalently, R_k^i can be defined as

$$R_k^i \propto \int_{380}^{780} E^i(\lambda) \cdot \rho^i(\lambda) \cdot s_k(\lambda) \mathrm{d}\lambda \qquad (2)$$

where $E^i(\lambda)$ is the spectrum of the illuminant falling upon colour stimulus i, $\rho^i(\lambda)$ the stimulus spectral reflectance, and $s_k(\lambda)$ the spectral absorption function of photoreceptor k [i.e., CIE standard observer (1931) colour matching functions $x(\lambda)$, $y(\lambda)$ and $z(\lambda)$ or Estévez–Hunt–Pointer fundamental primaries (Nayatani *et al.*, 1987)].

$R_{\max} = \max \{R_1, R_2, \ldots R_i, R_j, \ldots R_n\}$;

$R_{\min} = \min \{R_1, R_2, \ldots R_i, R_j, \ldots R_n\}$;

[β_{ij} → spectral channel M(G), γ_{ij} → spectral channel S(B).]

The additive constant has been included to avoid mathematical indetermination problems in totally black surrounds as Chichilnisky and Wandell also use in dichoptic asymmetric color matching experiments (Chichilnisky & Wandell, 1995), though a different value might have been chosen.

The features of this first-stage encoding are: (1) in the numerator, the lateral inhibition of the photoreceptors is represented by a non-linear substraction of the strengths of colour stimuli i and j in the same spectral domain, $\log(R_i + 1) - \log(R_j + 1)$, the choice of the logarithmic function being based on psychophysical evidence (Nayatani *et al.*, 1987; Hunt, 1991). Point j may be the nearest neighbour, an average of surrounding neighbours, or a suitably chosen reference surface, for example, a white surface. Later, we discuss the effects of choosing reference surfaces other than white on the invariance properties of the colour descriptors (Relativistic Colour Spaces section); (2) in the denominator, the effective colorimetric dynamic range (e.c.d.r.) ($R_{\max} - R_{\min}$) sets approximately the level of chromatic adaptation in that spectral domain. In a sense, this factor is influenced by the range or diversity of colour stimuli in the scene. Thus, under this encoding, we try to describe the main colour constancy mechanism: simultaneous mechanisms (numerator: lateral inhibition between photoreceptors of the same type) and adaptation mechanisms (denominator: scaling by the range of responses within one photoreceptor type across the image).

The following characteristics are implicit in the functions above.

Connection with the photometric rule

Human observers can assign the label "white (W)" ["black (BK)"] to colour stimulus i in a scene with n colour stimuli, characterized by:

$$\begin{aligned} &R_i = R_{\max} \textit{ and } G_i = G_{\max} \textit{ and} \\ &B_i = B_{\max} \Rightarrow i \equiv \text{label : white} \\ &R_i = R_{\min} \textit{ and } G_i = G_{\min} \textit{ and} \\ &B_i = B_{\min} \Rightarrow i \equiv \text{label : black.} \end{aligned} \qquad (3)$$

This property is known as the Photometric Rule, and implies that, as has been ascertained in several psychophysical experiments (Land, 1977; Bonato *et al.*, 1992; Li & Gilchrist, 1993; Szura & Gilchrist, 1994; Baüml, 1994), the perception of a colour stimulus i as "white" does not correspond with the theoretical description from the viewpoint of colorimetry ($R_{\max} = G_{\max} = B_{\max}$, i.e., $r_{\max} = g_{\max} = b_{\max} = 0.3333$). This is illustrated, for example, by Gilchrist in his psychophysical experiments and by Baüml in his experiments on subjective matching of an assumedly achromatic stimulus. So, for instance, in a chromatic environment formed by several Munsell samples of different brightness V and chroma C, but hues H 2.5, 5.0, 7.5, 10.0 BG, the white obtained by subjective matching shows a marked blue–green hue, even under different illuminants. This means that within the range of colours in the scene, R_W has comparatively smaller values than G_W and B_W, and so, colorimetrically, the perceived white presents a slight BG tint. Those experiments support the notion that we assign to stimulus i the label "white" when $R_i = R_{\max}$, $G_i = G_{\max}$, $B_i = B_{\max}$, even though $R_i{:}G_i{:}B_i \neq 1$. Besides, this encoding may use $R_{\max}$ as a reference for lateral inhibition in the R spectral channel even if $R_{\max}$ occurs for a surface that does not present the maximum values in the other channels. (For additional explanations, see the sections entitled "The problem of the presence of a white in the scene" and "*Relativistic colour spaces*".)

Thus, when defining the colour descriptors (α_{ij}, β_{ij}, γ_{ij}) we have taken into account how the visual system makes use of the photometric rule to perform a first-stage chromatic contrast processing.

Connection with previous theoretical models

When applying these colour descriptors, we must bear in mind the distinction between "achromatic" relativistic

spaces and "chromatic" relativistic spaces. In particular, we distinguish two possible achromatic references:

— Black reference: $R_j = R_{BK} = R_{min}$

$$\Rightarrow \alpha_{iBK} = \frac{\log(R_i + 1) - \log(R_{min} + 1)}{\log(R_{max} - R_{min} + 1)} \times 100 \quad (4)$$

— White reference: $R_j = R_W = R_{max}$

$$\Rightarrow \alpha_{iW} = \left[1 + \frac{\log(R_i + 1) - \log(R_{max} + 1)}{\log(R_{max} - R_{min} + 1)}\right] \times 100 \quad (5)$$

Taking into account the photometric rule, the colour descriptors (α_{ij}, β_{ij}, γ_{ij}) include, as a particular case, the concept of integrated reflectance ρ_k^i from the retinex-type algorithms (McCann *et al.*, 1976; Brainard & Wandell, 1986; Hurlbert, 1986):

$$\text{if } R_{min} = R_{BK} = 0 \text{ and } R_{max} = R_W \Rightarrow \alpha_{iBK} = \alpha_{iW} =$$

$$100 \frac{\log(R_i + 1)}{\log(R_W + 1)} \cong 100 \cdot \Gamma^i_{k=R} \quad (6)$$

$\Gamma^i{}_k$ being the logarithmic version of the integrated reflectance

$$\rho_k^i = \frac{R_k^i}{R_k^W} \longrightarrow \Gamma_k^i = \frac{\log(R_k^i)}{\log(R_k^W)}. \quad (7)$$

One of Land's original retinex algorithms (Land, 1977) uses the ratio $\log(R_k^i/R_k^W)$ as a colour descriptor, numerically different from $\log(R_k^i) / \log(R_k^W)$.

Example: center–surround paradigm

As an example, we describe the output of our first-stage colour encoding algorithm with a typical center–surround paradigm. Consider a white center–red surround paradigm, with the strength values in arbitrary units in the L(R), M(G) and S(B) spectral domains shown in Fig. 1.

If we compute the proposed colour descriptors, we obtain that the influence of the surround on the appearance of the center yields different brightness values in the different channels:

$$\alpha_{c-s} = \frac{\log(201) - \log(151)}{\log(200 - 150 + 1)} \times 100 = 7.28$$

$$\beta_{c-s} = \gamma_{c-s} = \frac{\log(201) - \log(26)}{\log(200 - 25 + 1)} \times 100 = 39.56. \quad (8)$$

Since the green and blue channels have larger responses than the red, a second stage opponent processing would assign the center a desaturated green colour.

Without the red surround, the white center would be chromatically encoded as:

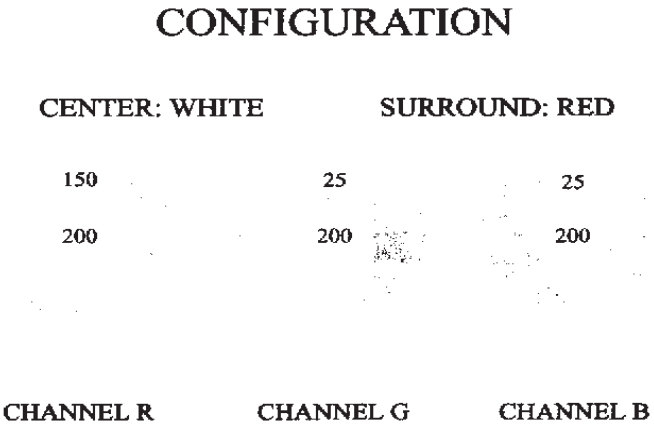

FIGURE 1. White center–red surround paradigm (see text for details).

$$\alpha_c = \beta_c = \gamma_c = \left[1 + \frac{\log(201) - \log(256)}{\log(201)}\right] \times 100 = 95.44 \quad (9)$$

using as a reference the equienergetic stimulus E [in our case, (255, 255, 255)]. In the same way, the isolated surround (without the center, that is) would be encoded as

$$\alpha_s = \left[1 + \frac{\log(151) - \log(256)}{\log(151)}\right] \times 100 = 89.48 \quad (10)$$

$$\beta_s = \gamma_s = \left[1 + \frac{\log(26) - \log(256)}{\log(151)}\right] \times 100 = 29.80.$$

Let us now re-scale the signals using the equienergetic reference E to see the global chromaticities and brightness, taking into account the influence of the neighbouring stimulus in the denominator —i.e., scaling the colour descriptors by the range of values in each spectral channel:

$$\alpha_c = \left[1 + \frac{\log(201) - \log(256)}{\log(200 - 150 + 1)}\right] \times 100 = 93.85 \quad (11)$$

$$\beta_c = \gamma_c = \left[1 + \frac{\log(201) - \log(256)}{\log(200 - 25 + 1)}\right] \times 100 = 95.32$$

$$\alpha_s = \left[1 + \frac{\log(151) - \log(256)}{\log(200 - 150 + 1)}\right] \times 100 = 86.57 \quad (12)$$

$$\beta_s = \gamma_s = \left[1 + \frac{\log(26) - \log(256)}{\log(200 - 25 + 1)}\right] \times 100 = 55.77.$$

These results show that the white center appears darker and greener than in absence of the surround, whereas the surround appears lighter and more desaturated than when viewed on its own.

Note that the differences between these signals are the values calculated at the beginning (7.28, 39.56, 39.56).

The mathematical model we propose for the first stage of colour processing is very simple, particularly when compared with the complex lateral interactions at the retinal level. Nonetheless, by adequately including an opponent second stage, we might obtain firmer conclusions on the validity of the first-stage model proposed. Even so, with this first-stage chromatic encoding and bearing in mind the aspects described, we outline below some ideas about two important questions.

The problem of the presence of a white stimulus in the scene

According to the photometric rule, the human visual system assigns the label "white" to colour stimuli i that fulfil the condition ($R_i = R_{max}$, $G_i = G_{max}$, $B_i = B_{max}$) even when, in general, $R_i{:}G_i{:}B_i \neq 1$. It is important to remark that in spite of ever-changing environmental conditions this rule is usually satisfied, i.e., such a "white" exists (Bonato *et al.*, 1992; Li & Gilchrist, 1993; Szura & Gilchrist, 1994).

In the extreme case that no stimulus in the scene can be labelled as "white" [see Eq. (3)], we have opted for referencing simultaneous contrast to the equienergetic stimulus E or ideal white, whenever it is indispensable. Then, the colour descriptors (α_{ij}, β_{ij}, γ_{ij}) would be expressed by:

$$\alpha_{iE} = \left[1 + \frac{\log(R_i + 1) - \log(R_E + 1)}{\log(R_{max} - R_{min} + 1)}\right] \times 100. \quad (13)$$

β_{ij} and γ_{ij} have similar expressions. We could reason in an analogous way for the black stimulus.

Note that this case represents a contour condition far more restrictive than the previous one, even though an absolute reference is employed. In the case of the equienergetic stimulus E we must bear in mind that its validity is restricted to isolated colours, whereas the photometric rule can be applied to related colours and is therefore better adapted to the usual contour conditions. Nevertheless, as we show below (Results and Discussion, Appendix) the selection of a white reference according to the photometric rule always yields better colour constancy than other white reference selections. Then, these results indicate that the human visual system applies the photometric rule as an additional adaptive factor to the ever-changing surround conditions to codify colour efficiently. Although the purpose of this model is not to reproduce human colour constancy exactly, we think that it would be interesting to make use some direct comparisons between this model and human perception.

Relativistic colour spaces

In a scene formed by n colour stimuli, it is possible to define n relativistic spaces according to the expression of the colour descriptors (α_{ij}, β_{ij}, γ_{ij}). That is, for every colour stimulus i in the scene, there are $n-1$ triplets (α_{ij}, β_{ij}, γ_{ij})$_{j=1,\ldots,n-1}$ associated to that stimulus i. In particular, when the reference of the relativistic space is the black stimulus (BK) we find the colour descriptors (α_{iBK}, β_{iBK}, γ_{iBK}). On the other hand, when the reference of the relativistic space is the white stimulus (W) we obtain colour descriptors (α_{iW}, β_{iW}, γ_{iW}). With the equienergetic reference, we would find (α_{iE}, β_{iE}, γ_{iE}).

For instance, we may suggest an alternative formulation for metamerism. Let us consider the relativistic space referred to colour stimulus (or hue) j. Colour stimulus i and j in the scene will be metameric when their receptoral absorptions are equal ($R_i = R_j$, $G_i = G_j$, $B_i = B_j$). With the chromatic encoding designed in this work, the colour descriptor triplet would be (α_{ij}, β_{ij}, γ_{ij}) = (0,0,0). With partial metamerism, that is, when $R_i = R_j$ but $G_i \neq G_j$ and $B_i \neq B_j$, the triplet would be (0, β_{ij}, γ_{ij}). We will discuss again this question in the next section, in the light of a series of results.

Other interesting question refers to the experimental results of Arend and co-workers (Arend & Reeves, 1986; Arend *et al.*, 1991). As stated in the Introduction, their papers show that the visual system makes use of colour stimuli in the scene, related to the same hue, to perform asymmetrical matching (*paper match*) trying to keep the appearance of a colour stimulus constant in spite of changes in the illuminant. This means that, if we were able to describe this experiment from the viewpoint of our chromatic encoding procedure, we would find that the colour descriptor triplets for stimulus i with reference to stimulus j, approximately related to the same hue, would show great stability under changes of the illuminant. It is important to remark that with a white or black reference, we would be in a more general case than when using the integrated reflectance, which yielded partial colour constancy under changes of the illuminant. Nonetheless, the results contributed by these scientists, and those we provide in the following section, show that there is useful additional information about colour constancy in relativistic colour spaces referred to as hues.

Now that we have introduced some general features of and questions arising from this first stage of a two-stage colour constancy algorithm (as we cannot forget that a second stage must exist, although we have not modelled it), we will now investigate experimentally the versatility or efficiency of this first-stage colour encoding. To this end, we implement our algorithm in a typical machine vision system. Then, we study the statistical stability of the colour descriptors under spectral changes of the illuminant, both in the case of achromatic relativistic spaces (black or white reference), and in hue related relativistic spaces.

RESULTS AND DISCUSSION

We perform a simulation to determine the efficiency of the designed colour descriptors under a range of standard illuminants, using Mondrian-like configurations. The simulations consist of the implementation of the proposed first-stage steps in a typical machine vision system (Jain, 1989).

We mean to carry out the aspects of the first-stage process on the optic sensor of the system (a CCD RGB camera, model SONY XC-711P). That is, we will consider the camera's spectral sensitivity curves, $s_k(\lambda)$

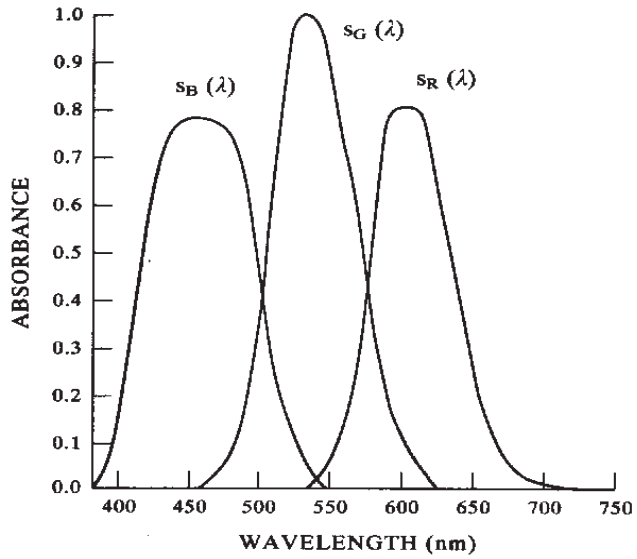

FIGURE 2. CCD-RGB camera's spectral sensitivity curves.

(Fig. 2), as the spectral absorption curves of this particular system of photoreceptors. The models based on this device are called quasi-physiological models. Taking into account the manufacturer's colorimetric calibration procedure and that the intensity dynamic range is 8 bits, that is, from 0 to 255 possible values of R_i, the transformation that goes from the colorimetric space RGB-CCD to the reference space CIE-1931 XYZ (equal-energy illuminant normalization) is:

$$\left[\begin{pmatrix} X \\ Y \\ Z \end{pmatrix}\right]_{\text{CIE-1931}} = \frac{100}{255}\left[\begin{pmatrix} 0.6259 & 0.2071 & 0.1670 \\ 0.4162 & 0.4787 & 0.1051 \\ 0.0007 & 0.0496 & 0.9497 \end{pmatrix}\right] \cdot \left[\begin{pmatrix} R \\ G \\ B \end{pmatrix}\right]_{\text{CCD}} \quad (14)$$

It is important to note that this implementation of our first-stage steps intends to simulate simply the complex lateral interaction processes that occur in the retina in the human visual system. Despite its simplicity, such an implementation on a machine vision system (MVS), with its technical limitations compared with the capabilities of the human visual system, should be of great interest due to the application of these devices to everyday industrial processes (Wallace, 1988).

We will now measure the degree of constancy of a MVS endowed with this algorithm, as well as test the different aspects we have outlined above. To do this, we will use two Mondrian patterns under a range of standard illuminants.

Experiment 1

In the first experiment, we compute the colour descriptors for Munsell samples in a Mondrian pattern under four different illuminants. We compare the constancy of descriptors using different references—white or black. We have considered a Mondrian pattern, composed of a set of ten Munsell samples of identical lightness $V = 6$, chroma or saturation $C = 6$, with the ten fundamental hues H 5.0 (*BP*, *B*, *BG*, *G*, *GY*, *Y*, *YR*, *R*, *RP*, *P*), placed on a black background. Actually, there are 12 well differentiated colours in the scene, if we include the white base of the Munsell samples (Fig. 3).

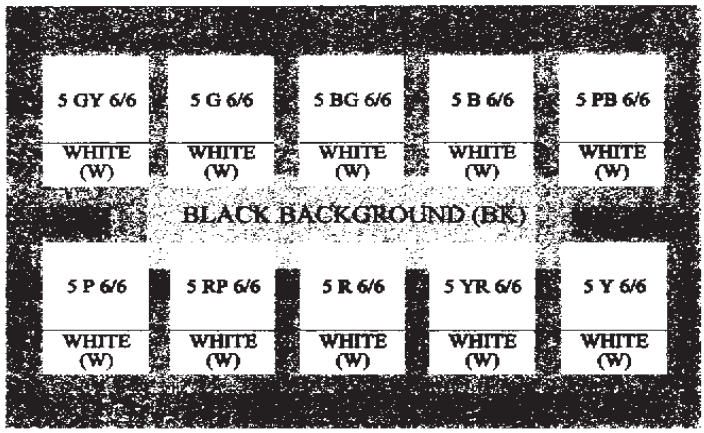

FIGURE 3. Spatial configuration of Munsell samples in Experiment 1.

The scene has been registered using four different standard illuminants (A, D32, D65 and C). The table of the maximum and minimum values in the three spectral domains provides information about how the CCD RGB camera records the chromaticity of the illuminant (Table 1). These values are related statistically to the parameters R_{max} and R_{min} that appear in the expression of the colour descriptors, which are taken from a colour quantization algorithm (Martínez-Verdú *et al.*, 1996) to make them statistically significant.

The change of the illuminant causes an "accordion effect" in the ordering of the intensity values (R_i, G_i, B_i) associated with each colour area i in the scene (Dannemiller, 1993; Martínez-Verdú *et al.*, 1996). In a way, the brightness of all colour areas is re-scaled. This effect is approximately equivalent to calculate RGB intensity ratios (Foster & Nascimento, 1994).

This shift in RGB intensity values may be seen as a colorimetric shift in the chromaticities of the Munsell samples, plotted in the CIE-(x, y) space (Fig. 4). If our MVS possessed colour constancy, the pseudo-elliptical

TABLE 1. Experiment 1: chromaticity capture of the illuminants A, D32, D65 and C by CCD-RGB camera

	Max (R) Min (R)	Max (G) Min (G)	Max (B) Min (B)
Illum. A	197	173	145
	13	8	12
Illum. D32	240	223	201
	18	9	16
Illum. D65	154	176	227
	12	8	21
Illum. C	164	184	248
	9	5	14

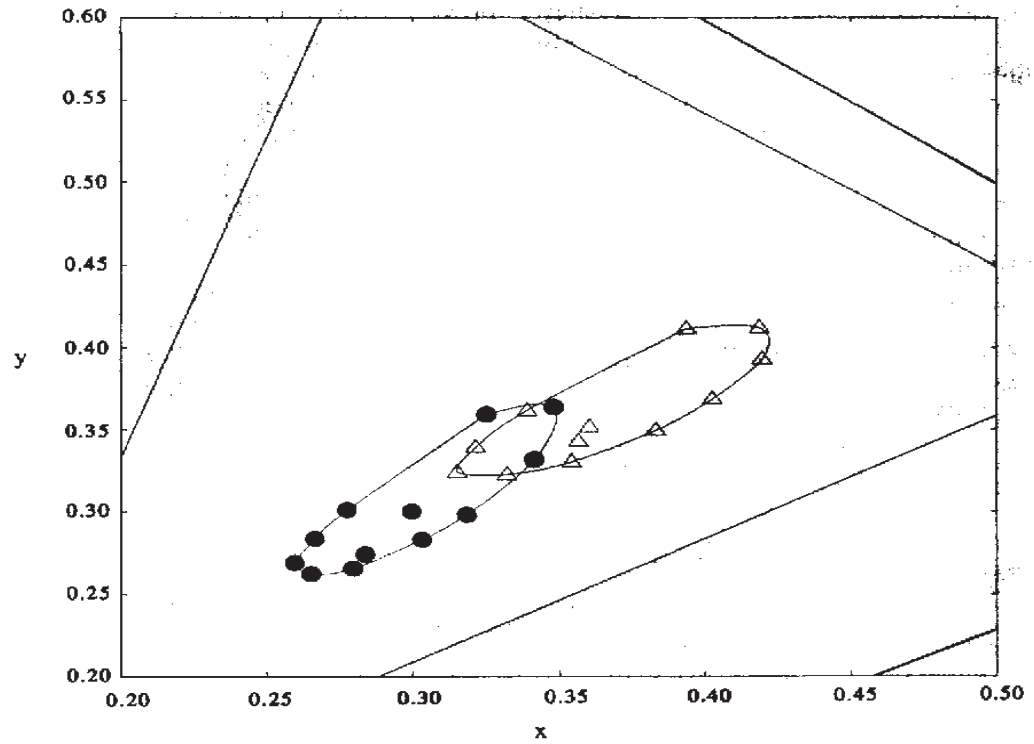

FIGURE 4. Chromatic encoding of colour samples in the first visual scene, using the CIE-1931 (x, y) diagram, according to the CCD-RGB colorimetric space: (●) samples under illuminant D65, (△) samples under illuminant A. Notice that the partial superposition of the pseudo-elliptical figures indicate partial colour constancy.

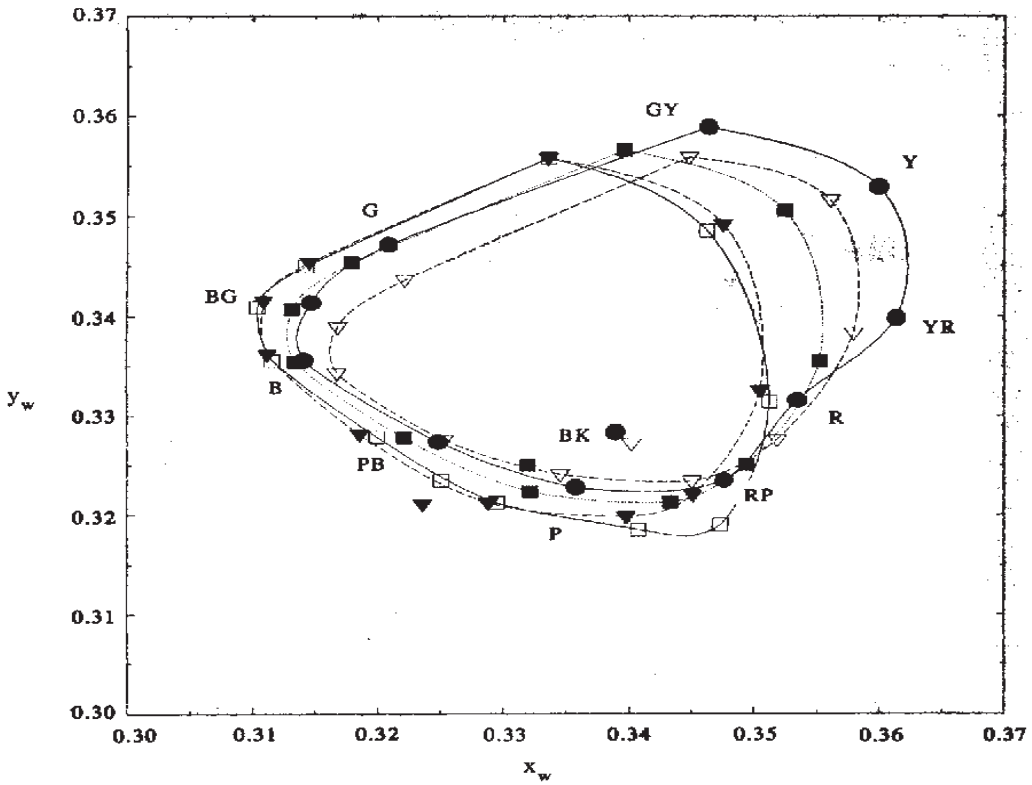

FIGURE 5. Representation of the statistical variance of the colour samples under spectral changes of the illuminant, as described by (x_{iW}, y_{iW}): (●) samples under illuminant A, (▽) samples under illuminant D32, (▼) samples under illuminant D65, (□) samples under illuminant C and (■) samples under average illuminant (A, D32, D65, C). Notice that the high degree of superposition of the pseudo-elliptical figures reflects an enormous compensation of the initial colorimetric shifts due to spectral changes of the illuminant.

figure formed by the Munsell samples of the system under a given illuminant would be almost completely superimposed on the pseudo-elliptical figure obtained with a different illuminant. Figure 4 demonstrates that without the first-stage analysis the MVS outputs show only partial colour constancy.

To demonstrate the statistical stability of the colour descriptors ($\alpha_{i\mathrm{W}}$, $\beta_{i\mathrm{W}}$, $\gamma_{i\mathrm{W}}$) and ($\alpha_{i\mathrm{BK}}$, $\beta_{i\mathrm{BK}}$, $\gamma_{i\mathrm{BK}}$) in the range of these four illuminants, we will represent two-dimensionally the ($x_{i\mathrm{W}}$, $y_{i\mathrm{W}}$, $z_{i\mathrm{W}}$) coordinates, defined as follows:

$$x_{i\mathrm{W}} = \frac{\alpha_{i\mathrm{W}}}{\alpha_{i\mathrm{W}} + \beta_{i\mathrm{W}} + \gamma_{i\mathrm{W}}}$$

$$y_{i\mathrm{W}} = \frac{\beta_{i\mathrm{W}}}{\alpha_{i\mathrm{W}} + \beta_{i\mathrm{W}} + \gamma_{i\mathrm{W}}} \qquad (15)$$

$$z_{i\mathrm{W}} = \frac{\gamma_{i\mathrm{W}}}{\alpha_{i\mathrm{W}} + \beta_{i\mathrm{W}} + \gamma_{i\mathrm{W}}}$$

($x_{i\mathrm{BK}}$, $y_{i\mathrm{BK}}$, $z_{i\mathrm{BK}}$) are obtained in an analogous way.

In the two-dimensional representation ($x_{i\mathrm{W}}$, $y_{i\mathrm{W}}$) (Fig. 5) and ($x_{i\mathrm{BK}}$, $y_{i\mathrm{BK}}$) (Fig. 6) we may observe, despite the change of the illuminant, a remarkable degree of superposition of the pseudo-elliptical figures defined by the coloured samples. If we compare this result with the previous ones, it can be observed that the colorimetric shifts of these pseudo-coordinates when the changes in the illuminant are far smaller than with the classic CIE-(x, y) chromatic coordinates (Fig. 4). Besides, it is easy to note that the statistical dispersion of colour descriptors ($\alpha_{i\mathrm{W}}$, $\beta_{i\mathrm{W}}$, $\gamma_{i\mathrm{W}}$) is smaller than that of descriptor ($\alpha_{i\mathrm{BK}}$, $\beta_{i\mathrm{BK}}$, $\gamma_{i\mathrm{BK}}$), and this is consistent with our intuition that referring the colour of the scene to the white stimulus yields better results than when a black reference is used, because a white stimulus always gives more information about the illuminant than a black stimulus according to their respective spectral reflectances.

On the issue of the photometric rule and the definition of "white" we present next the results of simulations in which the whites are chosen in four different ways (see Appendix):

- The equal-energy white ($\alpha_{i\mathrm{E}}$, $\beta_{i\mathrm{E}}$, $\gamma_{i\mathrm{E}}$) assigns the label white to the hypothetical stimulus (not necessarily realised in the scene) (255, 255, 255).
- The only-one-channel-maximum white or conventional model ($\alpha_{i\mathrm{W}}$, $\beta_{i\mathrm{W}}$, $\gamma_{i\mathrm{W}}$) assigns white to the surface that has the maximum value in each channel, even though that maximum value is not the same across all three channels. As written, this

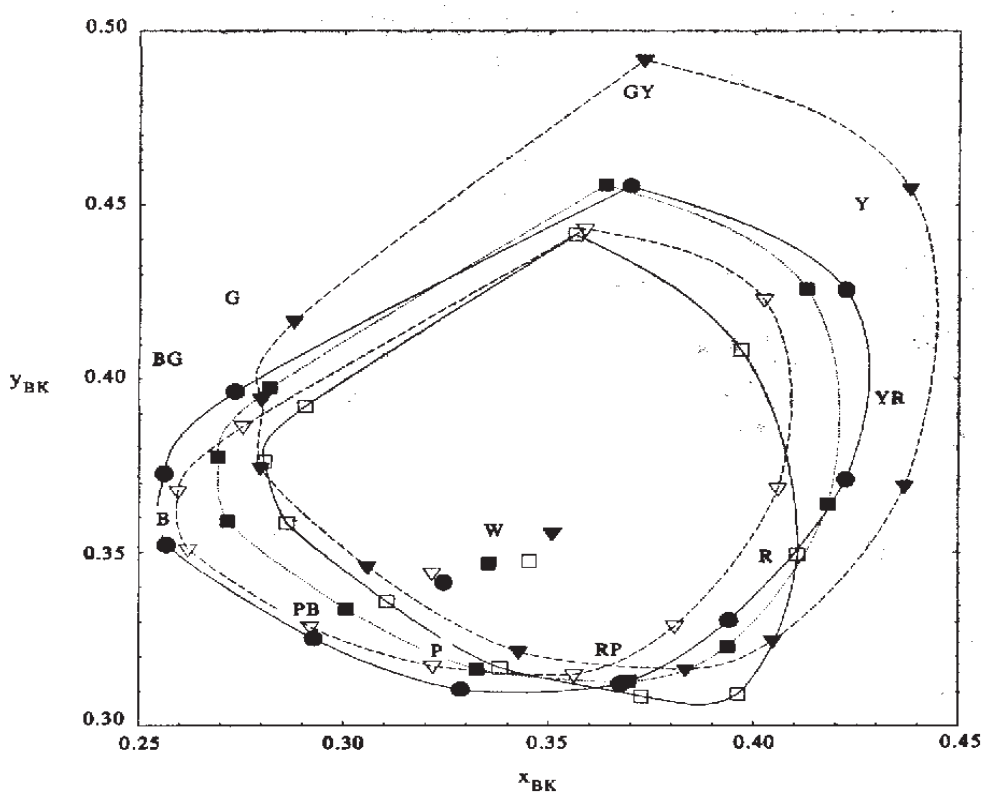

FIGURE 6. Statistical variance of the colour samples under spectral changes of the illuminant, as described by ($x_{i\mathrm{BK}}$, $y_{i\mathrm{BK}}$): (●) samples under illuminant A, (▽) samples under illuminant D32, (▼) samples under illuminant D65, (□) samples under illuminant C and (■) samples under average illuminant (A, D32, D65, C). Notice that the high degree of superposition of the pseudo-elliptical figures reflects an enormous compensation of the initial colorimetric shifts owing to spectral changes of the illuminant. Note also the difference in scale between this figure and the previous one, which shows the results using a white stimulus as a reference.

rule does not necessarily constrain the white to be the same surface in each channel as it is shown in Table A1;

- The all-channels-maximum white or pseudo-equal-energy white ($\alpha_{i\mathrm{WW}}$, $\beta_{i\mathrm{WW}}$, $\gamma_{i\mathrm{W}}$) finds the maximum value across all three channels and assigns white to be that same maximum value in each of the three channels.

- The without-white ($\alpha_{i\mathrm{Max}}$, $\beta_{i\mathrm{Max}}$, $\gamma_{i\mathrm{Max}}$) which chooses the maximum value of the non-whites in each channel.

In this last case, the effective colorimetric dynamical range, $R_{\max}-R_{\min}$, in each spectral domain will be affected. The photometric rule is implicit in ($\alpha_{i\mathrm{W}}$, $\beta_{i\mathrm{W}}$, $\gamma_{i\mathrm{W}}$) and ($\alpha_{i\mathrm{Max}}$, $\beta_{i\mathrm{Max}}$, $\gamma_{i\mathrm{Max}}$) because if white were present in a scene then ($\alpha_{i\mathrm{Max}}$, $\beta_{i\mathrm{Max}}$, $\gamma_{i\mathrm{Max}}$) would be transformed into ($\alpha_{i\mathrm{W}}$, $\beta_{i\mathrm{W}}$, $\gamma_{i\mathrm{W}}$); however, the photometric rule is not implicit in ($\alpha_{i\mathrm{E}}$, $\beta_{i\mathrm{E}}$, $\gamma_{i\mathrm{E}}$) and ($\alpha_{i\mathrm{WW}}$, $\beta_{i\mathrm{WW}}$, $\gamma_{i\mathrm{WW}}$).

In the next two-dimensional representation (Fig. 7) we now may observe a remarkable degree of superposition of the pseudo-elliptical figures defined by the coloured samples, despite the change of illuminant (D32 to C). Under the outlines of Creutzfeldt's relativistic model and photometric rule a high degree of colour constancy is shown in ($x_{i\mathrm{W}}$, $y_{i\mathrm{W}}$) and ($x_{i\mathrm{Max}}$, $y_{i\mathrm{Max}}$). On the other hand, this high degree of colour constancy is not present in ($x_{i\mathrm{E}}$,

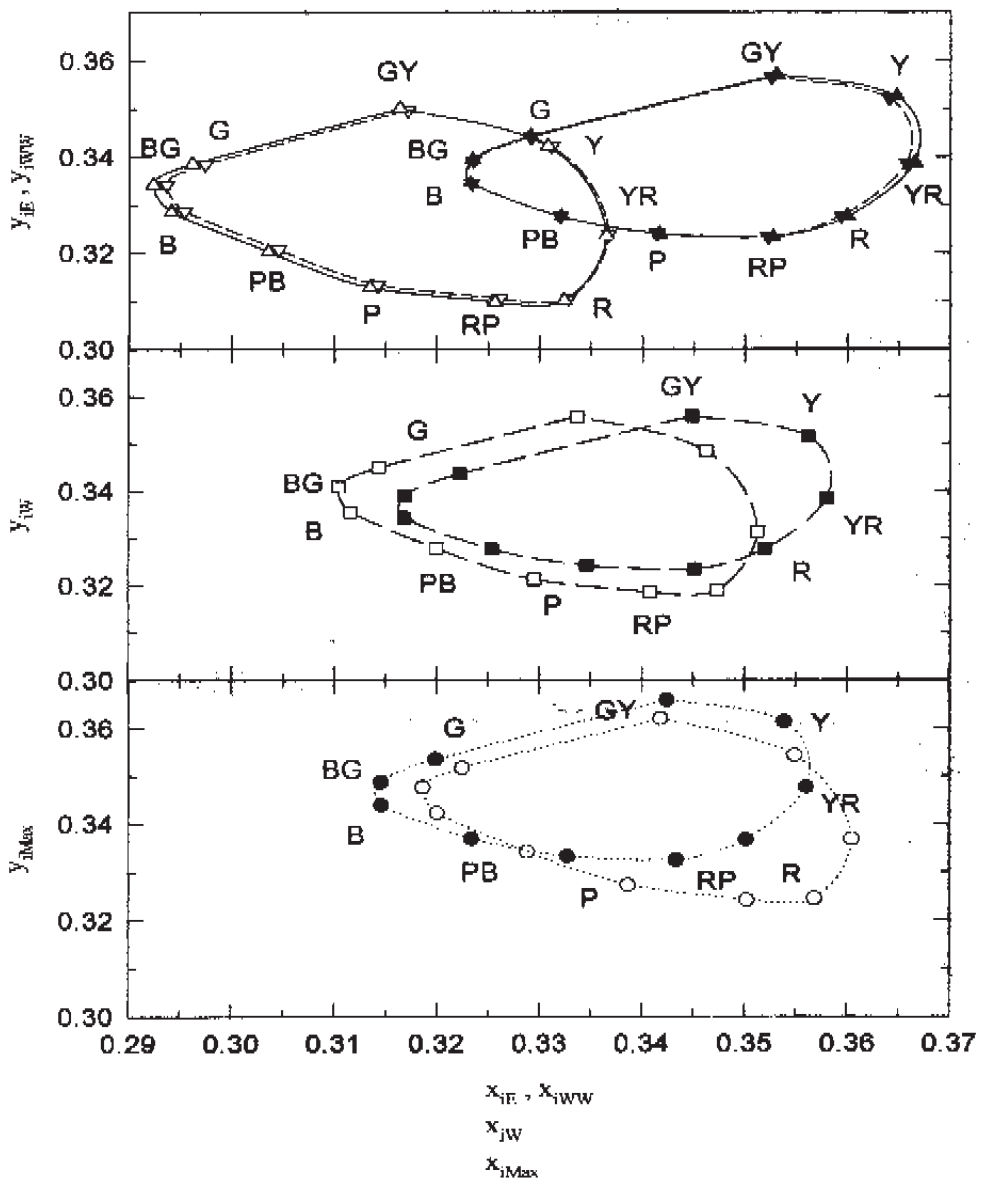

FIGURE 7. Representation of the statistical variance of the colour samples under spectral changes of the illuminant (D32, filled symbols to C, open symbols) according to different white references: (△) equal-energy white ($x_{i\mathrm{E}}$, $y_{i\mathrm{E}}$), (▽) all-channels-maximum-white or pseudo-equal-energy white ($x_{i\mathrm{WW}}$, $y_{i\mathrm{WW}}$), (□) only-one-channel-maximum white or conventional model ($x_{i\mathrm{W}}$, $y_{i\mathrm{W}}$), and (○) without-white ($x_{i\mathrm{Max}}$, $y_{i\mathrm{Max}}$).

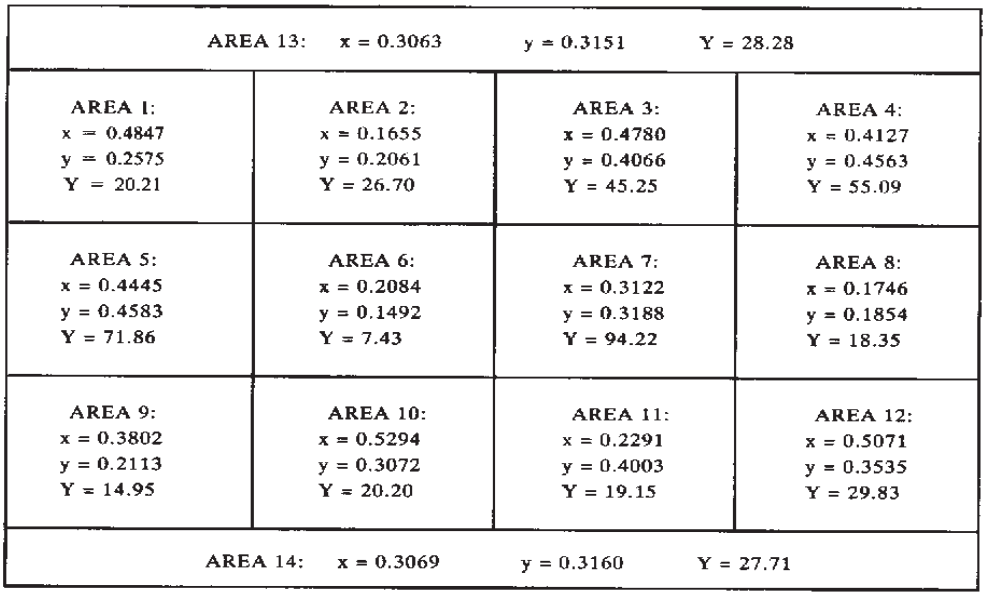

FIGURE 8. Spatial configuration of colour areas in Experiment 2, using the standard observer CIE-1931 with illuminant C.

y_{iE}) and ($x_{i_{WW}}$, y_{iWW}). The main reason is that these chosen white references do not give colorimetric information about the illuminant present in the scene. Therefore, if a white stimulus is not present in the scene, equal-energy white encoding in colour descriptors gives an intermediate degree of colour constancy.

Experiment 2

This experiment will confirm our previous results, and, in some respects, some results presented by Arend and co-workers (Arend & Reeves, 1986; Arend *et al.*, 1991). We will make use of the relativistic colour spaces referred to as hues. Unlike our former experiment, the samples in the Mondrian pattern (Fig. 8) were printed using an ink-jet printer ("printer" samples, model CANON BJC800), with the peculiarity that there is no stimulus in the scene that can be labelled as black. This will influence the computation of the colour descriptors (the effective colorimetric dynamical range, $R_{max}-R_{min}$, in each spectral domain will be affected).

We have registered this scene with a gamut of five different illuminants, with combinations of daylight (type CIE-C and CIE-D65), and reddish light (type CIE-A) and typical fluorescent light. The recording of maximum and minimum values in the three spectral domains—unrelated to the values R_{max} and R_{min} employed to calculate the colour descriptors—provides insight about the way the CCD RGB records the illuminants' chromaticities. (Table 2).

Once we know the xyY values (Fig. 8) and intensity values (R_i, G_i, B_i) we may conclude that area number seven is the white stimulus in the scene, whereas where there is no coloured area we might label black. Area number 6 (dark-purplish blue) has minimum values both in channels R and G (that is, $R_6 = R_{min}$ and $G_6 = G_{min}$), whereas area number 10 (scarlet) has a minimum value in channel B, (that is, $B_{10} = B_{min}$). Following the procedure devised in our previous experiment, we measure the system's degree of colour constancy by studying the statistical variation of the colour descriptors ($\alpha_{i7=W}$, $\beta_{i7=W}$, $\gamma_{i7=W}$) in the two-dimensional representation defined by the pseudo-chromatic coordinates (x_{iW}, y_{iW}) (Fig. 9). If we compare these results with the analogous representation in the CIE-(x, y) space (Fig. 10), we observe that, again, the colorimetric shifts have been reduced, as is shown by the degree of superposition of the pseudo-elliptical figures for each illuminant.

To give an example of the functionality of the first-stage mechanism proposed, we proceed now to apply it to the case of relativistic colour spaces referred to as hue. To this end, using the same set of five illuminants, we have computed the colour descriptors for all colour samples in the scene but taking as reference a chromatic sample. We have chosen, for instance, areas 8 (blue) and 3 (orange), since the first one is representative of samples 2, 6, 8 and

TABLE 2. Experiment 2: chromaticity capture of the many illuminants by CCD RGB camera

	Max (R) Min (R)	Max (G) Min (G)	Max (B) Min (B)
Illum. 1: indirect daylight (CIE-C)	226	230	250
	32	20	59
Illum. 2: indirect daylight reddish light	241	232	234
(CIE-A)	36	21	48
Illum. 3: reddish light (CIE-A)	246	236	231
	36	27	58
Illum. 4: reddish light indirect daylight	220	198	200
	38	26	44
Illum. 5: indirect daylight fluorescent	188	198	250
light	32	22	54

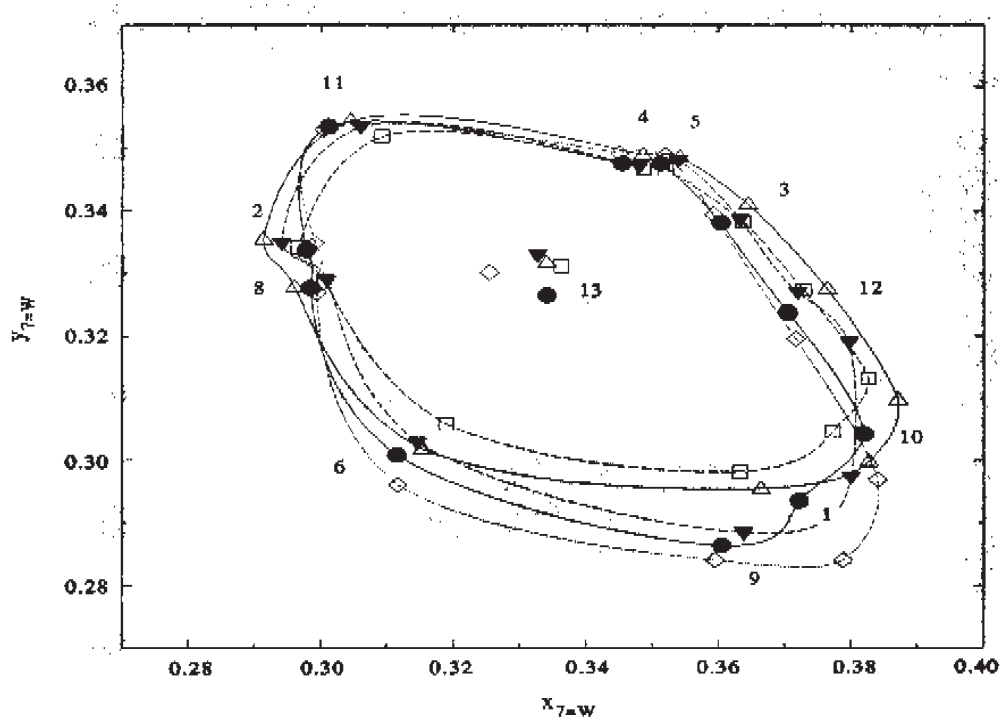

FIGURE 9. Statistical variance of the colour areas under spectral changes of the illuminant, as encoded by $(x_{i7=W}, y_{i7=W})$: (●) colour areas under illuminant 1, (▼) colour areas under illuminant 2, (□) colour areas under illuminant 3, (△) colour areas under illuminant 4 and (◇) colour areas under illuminant 5. Notice that the high degree of superposition of the pseudo-elliptical figures reflects an enormous compensation of the initial colorimetric shifts due to spectral changes of the illuminant.

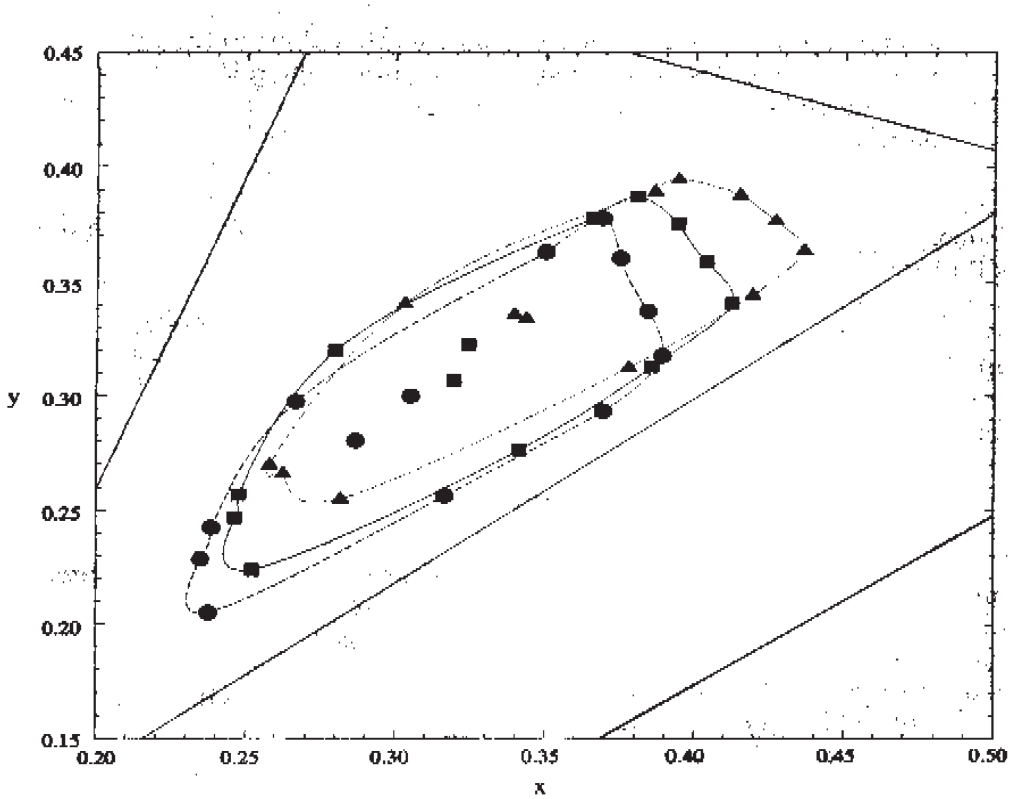

FIGURE 10. Chromatic encoding of the colour areas in the scene used in Experiment 2, using the CIE-1931 (x, y) diagram, in accordance with the colorimetric space CCD-RGB: (■) colour areas under illuminant 1, (▲) colour areas under illuminant 3 and (●) colour areas under illuminant 5. Note that partial colour constancy is achieved, as there is a partial superposition of the pseudo-elliptical figures defined by the colour areas under the same illuminant.

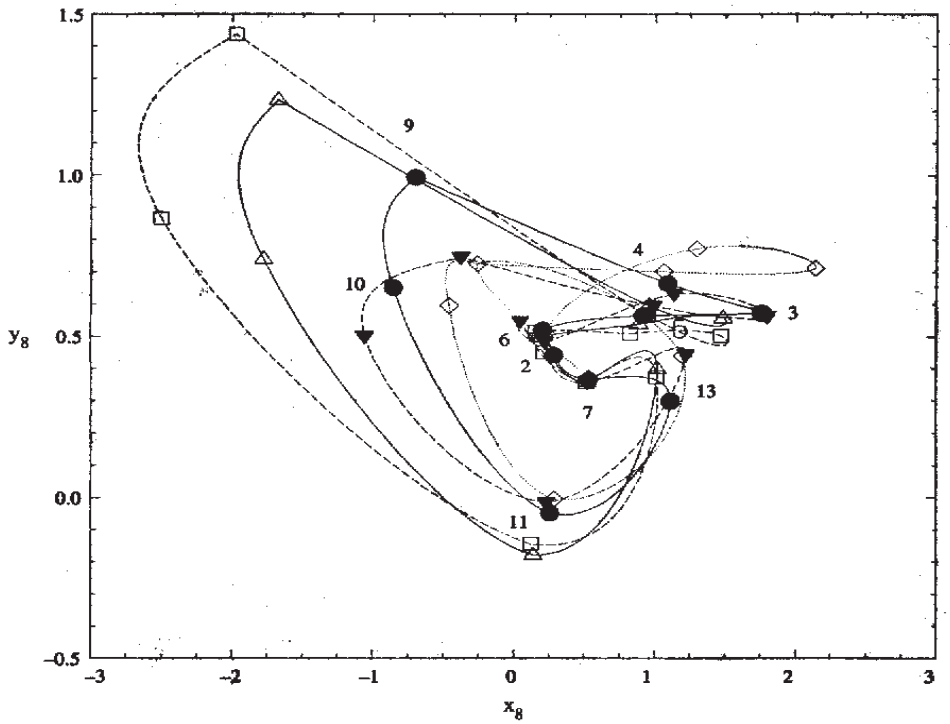

FIGURE 11. Enlarged representation of the statistical variance of the colour areas under spectral changes of the illuminant, as encoded by (x_{i8}, y_{i8}): (●) colour areas under illuminant 1, (▼) colour areas under illuminant 2, (□) colour areas under illuminant 3, (△) colour areas under illuminant 4 and (◇) colour areas under illuminant 5. (See text.)

11—hues from the medium-short wavelength region of the spectrum—and the second is representative of the set defined by samples 1, 4, 5, 9 10, 11 and 12—hues from the medium-long wavelength range. In the light of the two-dimensional representations (x_8, y_8) and (x_3, y_3), evidently we do not reproduce the pseudo-elliptical figures as in the case of achromatic relativistic space—black and white reference, respectively—as the distribution of the samples is far more irregular.

In the case of the relativistic space referred to as stimulus 8 (blue) there is a large dispersion in the first-stage values of the samples under the five illuminants—so much so that plotting all the values in one diagram reveals an almost unintelligible tangle of data. Colour areas 1 and 12 undergo particularly large shifts under this gamut of illuminants, and are not displayed. Nevertheless, with a change of scale, the results are more satisfactory (Fig. 11). (i) The reciprocity of the stability under changes of illuminant with respect to area 7 (white) is complete: area 7 presents an excellent stability, that is, the points for area 7 are superposed. (ii) Areas 2, 6 and 11, related to area 8 according to what we have said above, also show an excellent stability under the range of illuminants employed, perhaps slightly lower than that of area 11. However, in addition, there are some areas unrelated in hue (areas 3, 4, 5 and 13) that show good stability under changes of the illuminant. On the other hand, taking into account our former interpretation of metamerism, with this representation area 11 is close to the point (0,0), which represents a total or partial metameric colour to the reference employed.

Regarding the relativistic space referred to as sample 3 (orange), again the first complete representation is practically unintelligible. Even so, it is observed that areas 2 and 13 are markedly unstable under changes in the illuminant when the reference is colour area 3. Enlarging this graph, we again obtain satisfactory results (Fig. 12). Thus, in the first place, the reciprocity with area 7 (white) is again excellent. Also, areas 9, 10 and 12, related in hue, show good stability under spectral changes in the illuminant. To a lesser degree, this happens also with areas 1, 4 and 5. In addition, areas 6 and 11, unrelated in hue, show a marked stability.

It seems, therefore, that relativistic colour spaces referred to as hues also contain additional information about constant relationships between colour stimuli under spectral changes in the illuminant. In a sense, the requisites for chromatic asymmetrical matching (*paper match*) in the experiments of Arend and co-workers (Arend & Reeves, 1986; Arend *et al.*, 1991) are based on the fact that the colorimetric relationships of the matching stimuli with neighbouring stimuli, approximately related in hue, provide useful information to achieve good matching under changes of the illuminant. This is consistent with the results obtained in our experiment, within the limitation of our particular system—quality of colour reproduction and, above all, the shape of the spectral sensitivity curves $s_\mu(\lambda)$.

Although the model is intended to by as physiologi-

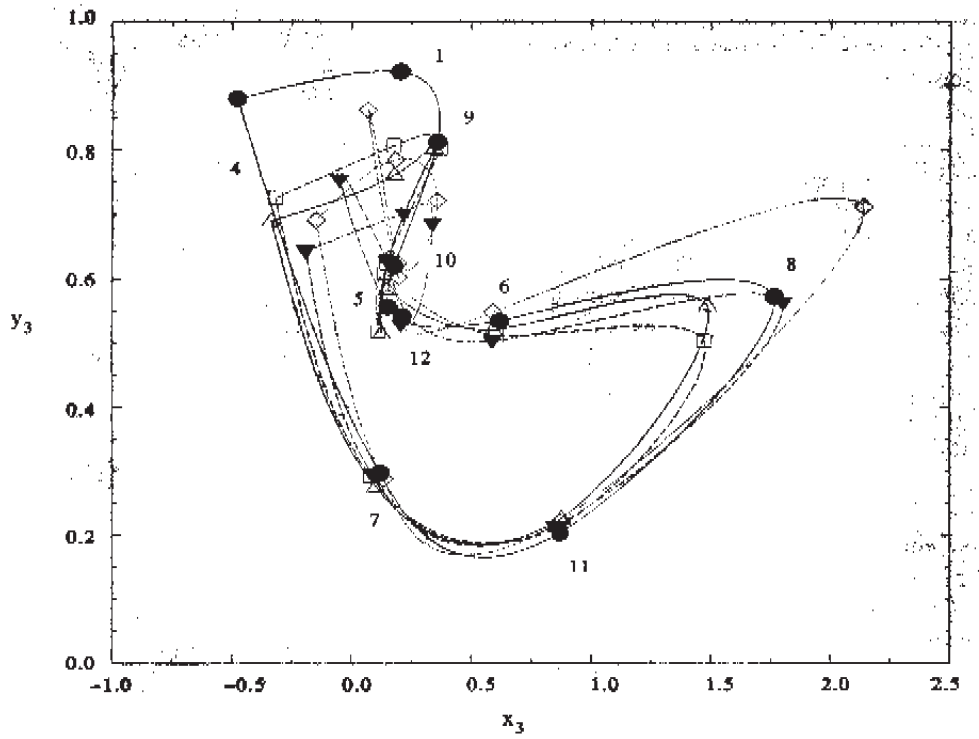

FIGURE 12. Enlarged representation of the statistical variance of the colour areas under spectral changes of the illuminant, as encoded by (x_{i3}, y_{i3}): (●) colour areas under illuminant 1, (▼) colour areas under illuminant 2, (□) colour areas under illuminant 3, (△) colour areas under illuminant 4 and (◇) colour areas under illuminant 5. (See text.)

cally plausible as computationally effective, it is not simple to compare directly its matching failures with those found in human observers due to some differences between the spectral channels of a MVS and the HVS, and in the simplicity of the implemented model as compared with the computational and architectural neural complexity of the HVS.

CONCLUSIONS

In this work, we have used the concepts of a relativistic model for chromatic induction (Creutzfeldt *et al.*, 1990) to propose a process that simulates the first stage of colour processing in the human visual system. As described by the model for chromatic induction, such a simulation takes into account the relative brightness within the three spectral domains [long (L or R), medium (M or G) and short (S or B)]. It also makes use of certain concepts based on psychophysical evidence, such as the photometric rule (lightness anchoring rule) and the control of chromatic adaptation. This first-stage process is described mathematically by means of colour descriptors $(\alpha_{ij}, \beta_{ij}, \gamma_{ij})$.

Although the first-stage process proposed cannot completely encompass all the complex neuronal interactions within the retina, it may reproduce the most important features of chromatic encoding at this level, and so it is interesting when implemented in a MVS. This interest lies in the use of relatively unrestrictive contour conditions, such as the application of the photometric rule to detect white and black stimuli.

As an application of the functionality of this first-stage mechanism through colour descriptors $(\alpha_{ij}, \beta_{ij}, \gamma_{ij})$, we have focused our work on problems related to colour constancy. From this viewpoint, we have distinguished between "achromatic" relativistic spaces—referred to as white $(\alpha_{i\mathrm{W}}, \beta i_{\mathrm{W}}, \gamma_{i\mathrm{W}})$ or a black $(\alpha_{i\mathrm{BK}}, \beta_{i\mathrm{BK}}, \gamma_{i\mathrm{BK}})$ stimulus—and "chromatic" relativistic spaces, referred to as hues. To this end, we have performed two simulation experiments, implementing this mechanism in a typical machine vision system.

The results of the first experiment show that the first-stage mechanism minimizes the colorimetric shifts due to spectral changes in the illuminant (Figs 5 and 6), if compared with the initial chromatic shifts in the classical colorimetric coordinates (Fig. 4). Moreover, we observe that, if we compare an additive chromatic encoding—based on a black reference—with a subtractive chromatic encoding—based on a white reference—the latter shows smaller statistical variation under changes in the illuminant than the former.

The choice of the white reference in colour constancy is generally a critical point. We have shown that a white that follows the photometric rule yields better colour constancy results than other possible white references (equal-energy white, etc.; Fig. 7). It is important to emphasize that if the visual system, human or machine, relies on an absolute reference that is not actually present in the scene, some useful colorimetric information about

the illuminant is missed. However, the photometric rule retrieves the information missed, achieving in this way a noteworthy colour constancy.

On the other hand, in accordance with the ideas about relativistic spaces referred to hues we have discussed, the results of our second experiment suggest that, in agreement with results reported by related investigations, there is useful additional information about colour constancy—that is, about the invariability of certain parameters under changes in the illuminant—in these not so common relativistic spaces. This leads us to inquire whether, in a sense, the human visual system makes use of part of this information, and, if it does, how this is accomplished. In the same way, this question must be asked from the field of machine vision for future application of the first-stage mechanism in machine vision systems.

Finally, we must remember that a complete colour constancy algorithm ought to consist of two stages at least. As we say in the Introduction, a first-stage mechanism like the one simulated in this work by means of a model for chromatic induction, already yields a small statistical variability under spatial changes of the illuminant. The second stage, necessary to build a chromatic perceptual space (by means of opponent processes, for instance) further supports the partial invariance of certain chromatic parameters thanks to new perceptual chromatic variables. In the case of the HVS, such a second stage would be well described by means of opponent processes. Nevertheless, in MVS it is possible to study different second-stage processes, based either on human psychophysical evidence or on new ideas and viewpoints, as yet undeveloped.

REFERENCES

Arend, L. (1993). How much does illuminant color affect unattributed colors? *Journal of the Optical Society of America A, 10*, 2134–2147.

Arend, L. & Reeves, A. (1986). Simultaneous color constancy. *Journal of the Optical Society of America A, 3*, 1743–1751.

Arend, L. E.Jr., Reeves, A. & Goldstein, R. (1991). Simultaneous color constancy: papers with diverse Munsell values. *Journal of the Optical Society of America A, 8*, 661–672.

Baüml, K.-H. (1994). Color appearance: effects of illuminant changes under different surface collections. *Journal of the Optical Society of America A, 11*, 531–542.

Baüml, K.-H. (1995). Illuminant changes under different surface collections: examining some principles of colour appearance. *Journal of the Optical Society of America A, 12*, 261–271.

Blackwell, K. T. & Buchsbaum, G. (1988). Quantitative studies of color constancy. *Journal of the Optical Society of America A, 5*, 1772–1780.

Bonato, F., Gilchrist, A. L. & Li, X. (1992). The anchoring rule for lightness perception under minimal conditions. *Investigative Ophthalmology and Visual Science, 33*, 1258.

Brainard, D. H. & Wandell, B. A. (1986). Analysis of the retinex theory of color vision. *Journal of the Optical Society of America A, 3*, 1651–1661.

Brill, M. H. (1993). Can color-space transformation improve color computations other than von Kries? *Proceedings of the SPIE Optical Engineering, 1993*, 485–492.

Chichilnisky, E.-J. & Wandell, B. A. (1995). Photoreceptor sensitivity changes explain color appearance shifts induced by large uniform backgrounds in dichoptic matching. *Vision Research, 35*, 239–254.

Cornelissen, F. W. & Brenner, E. (1995). Simultaneous colour constancy revisited: an analysis of viewing strategies. *Vision Research, 35*, 2431–2448.

Craven, B. J. & Foster, D. H. (1992). An operational approach to colour constancy. *Vision Research, 32*, 1359–1366.

Creutzfeldt, O., Lange-Malecki, B. & Dreyer, E. (1990). Chromatic induction and brightness contrast: a relativistic color model. *Journal of the Optical Society of America A, 7*, 1644–1654.

Creutzfeldt, O., Lange-Malecki, B. & Wortmann, K. (1987). Darkness induction, retinex and cooperative mechanisms in vision. *Experimental Brain Research, 67*, 270–283.

Creutzfeldt, O., Lee, B. & Valberg, A. (1983). Color and brightness signals of parvocellular lateral geniculate neurons. *Experimental Brain Research, 63*, 21–34.

Dannemiller, J. L. (1993). Rank orderings of photoreceptor photon catches from natural objects are nearly illuminant-invariant. *Vision Research, 33*, 131–140.

D'Zmura, M. & Iverson, G. (1994). Color constancy. III. General linear recovery of spectral descriptions for lights and surfaces. *Journal of the Optical Society of America A, 11*, 2389–2400.

Fechner, G. T. (1890). *Elemente der psychophysik*. Amsterdam: Basset. Reprinted in 1964.

Finlayson, G. D., Drew, H. S. & Funt, B. V. (1994). Spectral sharpening: sensor transformations for improved color constancy. *Journal of the Optical Society of America A, 11*, 1553–1563.

Foster, D. H. & Nascimento, S. M. C. (1994). Relational colour constancy from invariant cone-excitation ratios. *Proceedings of the Royal Society, London, B, 257*, 115–121.

Funt, B. V. & Finlayson, G. D. (1995). Color constant color indexing. *IEEE Transactions on Pattern Analysis and Machine Intelligence (PAMI), 17*, 522–529.

Healey, G. & Slater, D. (1994). Global color constancy: recognition of objects by use of illumination-invariant properties of color distributions. *Journal of the Optical Society of America A, 11*, 3003–3010.

Hunt, R. W. G. (1979). Measures of colour appearance in colour reproduction. *Color Research and Application, 4*, 39–43.

Hunt, R. W. G. (1991). Revised colour-appearance model for related and unrelated colours. *Color Research and Application, 16*, 146–165.

Hurlbert, A. (1986). Formal connections between lightness algorithms. *Journal of the Optical Society of America A, 3*, 1684–1693.

Hurvich, L. M. & Jameson, D. (1964). Theory of brightness and color contrast in human vision. *Vision Research, 4*, 135–154.

Jain, A. J. (1989). *Fundamentals of digital image processing*. New York: Prentice Hall.

Jin, E. W. & Shevell, S. K. (1996). Color memory and color constancy. *Journal of the Optical Society of America A, 13*, 1981–1991.

Krauskopf, J., Zaidi, Q. & Mandler, M. B. (1986). Mechanisms of simultaneous color induction. *Journal of the Optical Society of America A, 3*, 1752–1757.

von Kries, J. (1905). Die Gesichtsewpfindungen. In Nagel, W. (Ed.), *Handbuch der physiologie des menschen* (Vol. 3, pp. 109–282). Braünschweig.

Land, E. H. (1977). The retinex theory of color vision. *Scientific American, 237*, 108–128.

Land, E. H. (1986). Recent advances in retinex theory. *Vision Research, 26*, 7–21.

Land, E. H. & McCann, J. (1971). Lightness and retinex theory. *Journal of the Optical Society of America, 61*, 1–11.

Li, X. & Gilchrist, A. L. (1993). Geometric configuration and anchoring of surface lightness. *Investigative Ophthalmology and Visual Science, 34*, 748.

Lucassen, M. P. & Walraven, J. (1993). Quantifying color constancy: evidence for nonlinear processing of cone-specific contrast. *Vision Research, 33*, 739–757.

Lucassen, M. P. & Walraven, J. (1996). Color constancy under natural and artificial illumination. *Vision Research, 37*, 2699–2711.

Luo, M. R., Gao, X. W. & Scrivener, S. A. R. (1995). Quantifying colour appearance. Part V. Simultaneous contrast. *Color Research and Application, 20*, 18–28.

Mach, E. (1866). Über die Wirkung der räumlichen Veteilung des

Lichtreises aud die Netzhaut. *Sitzungsber Wiener Akad., 54*, 131–141. In Ratliff, F. (Ed.) *Mach bands*. San Francisco: Holden Day (1965).
Maloney, M. L. (1994). Color appearance and the control of chromatic adaptation. *Perception*, 23 (Suppl.), 7. Conference Paper. ECVP'94 (Eindhoven, Netherlands).
Maloney, L. T. & Wandell, B. A. (1986). Color constancy: a method for recovering surface spectral reflectance. *Journal of the Optical Society of America A, 3*, 29–33.
Martínez-Verdú, F. M., Arnau, V., Malo, J., Felipe. A. & Artigas, J. M. (1996). A new chromatic codification for machine vision practically invariant to the change of the illuminant. *Journal of Optics (Paris), 27*, 171–181.
McCann, J., McKee, S. P. & Taylor, T. H. (1976). Quantitative studies in retinex theory: a comparison between theoretical predictions and observer responses to the "color Mondrian" experiments. *Vision Research, 16*, 445–458.
Nayatani, Y., Hashimoto, K., Takahama, K. & Sobagaki, H. (1987). A nonlinear color–appearance model using Estévez–Hunt–Pointer primaries. *Color Research and Application, 12*, 231–242.
Singer, B. & D'Zmura, M. (1995). Contrast gain control: a bilinear model for chromatic selectivity. *Journal of the Optical Society of America A, 12*, 667–685.
Szura, J. E. & Gilchrist, A. L. (1994). Lightness anchoring of surfaces seen through an aperture in a complex display. *Investigative Ophthalmology and Visual Science, 35*, 2165.
Takasaki, H. (1969). Von Kries coefficient law applied to subjective color change induced by background color. *Journal of the Optical Society of America, 59*, 1370–1376.
Valberg, A., Lee, B. & Tryti, J. (1987). Simulation of responses of spectrally opponent neurons in the macaque lateral geniculate nucleus to chromatic and achromatic light stimuli. *Vision Research, 27*, 867–882.
Valberg, A. & Lange-Malecki, B. (1990). Colour constancy in Mondrian patterns: a partial cancellation of physical chromaticity shifts by simultaneous contrast. *Vision Research, 30*, 371–380.
Wallace, A. M. (1988). Industrial applications of computer vision since 1982. *IEE Proceedings Part E, 135*, 117–136.
Walraven, J. (1976). Discounting the background—the missing link in the explanation of chromatic induction. *Vision Research, 13*, 289–295.
Walraven, J., Benzschawel, T. L. & Rogowitz, B. E. (1987). Color-constancy interpretation of chromatic induction. *Die Farbe, 34*, 269–273.
Webster, J. A. & Mollon, J. D. (1993). The influence of contrast adaptation on color appearance. *Vision Research, 34*, 1993–2020.
Worthey, J. A. (1985). Limitations of colour constancy. *Journal of the Optical Society of America A, 2*, 1014–1026.
Worthey, J. A. & Brill, M. H. (1986). Heuristic analysis of von Kries color constancy. *Journal of the Optical Society of America A, 3*, 1708–1712.
Wyszecki, G. (1986). Color appearance. In Boff, K. R., Kaufmann, L. and Thomas, J. P. (Eds), *Handbook of human performance* (pp. 1–57). New York: Wiley.
Wyszecki, G. & Stiles, W. S. (1982). *Color science: concepts and methods; quantitative data and formulae* (2nd edn). New York: Wiley.

Acknowledgements—We thank two anonymous reviewers for their constructive criticism of this manuscript.

APPENDIX

Numerical example

The first numerical example is referred to in the results of Fig. 7, on the possible white reference selections for our colour descriptors calculation. Let us remember that the scene was a Mondrian pattern (Fig. 3) composed of ten Munsell chips of identical lightness V = 6, chroma or saturation C = 6, with the ten fundamental hues H 5.0 (R, YR, Y, GY, G, BG, B, PB, P, RP) placed against a black background. This scene was illuminated under two different lights maintaining approximately the same illumination: type D32 (reddish) and type C (bluish). After having captured the six RGB images and performing a segmentation/colour-quantization algorithm on colour surfaces, the scene is encoded into grey levels as shown in Table A1.

TABLE A1. Gray levels of Munsell chips under illuminant type D32

	R_i (σ_R)	G_i (σ_G)	B_i (σ_B)
Illum. D32			
GY	108.96 (0.65)	116.01 (0.59)	51.39 (1.29)
G	97.07 (0.61)	120.25 (0.66)	97.26 (1.04)
BG	96.62 (0.63)	121.35 (0.59)	119.68 (0.80)
B	102.86 (0.65)	121.54 (0.61)	136.50 (0.75)
PB	123.42 (0.64)	117.25 (0.66)	141.50 (0.85)
P	142.45 (0.59)	112.63 (0.56)	131.82 (0.97)
RP	155.65 (0.59)	105.16 (0.66)	108.25 (1.06)
R	154.58 (0.54)	101.34 (0.64)	84.72 (1.11)
YR	150.29 (0.50)	105.69 (0.50)	61.39 (1.30)
Y	132.64 (0.52)	114.76 (0.62)	48.70 (1.28)
BK	33.04 (1.42)	27.08 (1.14)	27.04 (1.32)
W	234.01 (5.27)	213.34 (6.15)	193.97 (5.36)
Illum. C			
GY	58.05 (0.63)	81.96 (0.65)	62.34 (1.36)
G	57.18 (0.70)	91.61 (0.78)	119.38 (1.00)
BG	67.31 (0.85)	100.61 (0.85)	179.63 (0.94)
PB	80.39 (0.71)	97.12 (0.78)	192.60 (1.05)
P	80.28 (0.70)	77.88 (0.76)	158.85 (0.98)
RP	89.24 (0.70)	72.14 (0.74)	134.27 (0.98)
R	86.84 (0.60)	65.32 (0.68)	108.09 (1.07)
YR	86.85 (0.82)	73.12 (0.88)	82.29 (1.29)
Y	76.38 (0.62)	85.07 (0.73)	65.41 (1.12)
BK	17.58 (0.67)	18.25 (0.91)	29.97 (1.68)
W	146.23 (5.44)	160.26 (6.15)	229.88 (7.06)

There are four ways to solve the problem of the white reference selection: equal-energy white (α_{iE}, β_{iE}, γ_{iE}), only-one-channel-maximum white or conventional model (α_{iW}, β_{iW}, γ_{iW}), all-channels-maximum white or pseudo-equal-energy white (α_{iWW}, β_{iWW}, γ_{iWW}), and, without-white (α_{iMax}, β_{iMax}, γ_{iMax}). With each choice we will obtain the following results:

- With the equal-energy white, $R_{max} = R_W$, $G_{max} = G_W$, $B_{max} = B_W$, $R_{min} = R_{BK}$, $G_{min} = G_{BK}$, $B_{min} = B_{BK}$ under both illuminations. Then

$$\alpha_{iE} = \left[1 + \frac{\log(R_i + 1) - \log(255 + 1)}{\log(R_W - R_{BK} + 1)}\right] \times 100 \qquad \text{(A1)}$$

- With the only-one-channel or conventional model: $R_{max} = R_W$, $G_{max} = G_W$, $B_{max} = B_W$, $R_{min} = R_{BK}$, $G_{min} = G_{BK}$, $B_{min} = B_{BK}$ under both illuminations. Then

$$\alpha_{iW} = \left[1 + \frac{\log(R_i + 1) - \log(R_W + 1)}{\log(R_W - R_{BK} + 1)}\right] \times 100 \qquad \text{(A2)}$$

- With the all-channels-maximum white or pseudo-equal-energy white: for example, under D32 illuminant, $R_W = 234.01 = R_{max} > G_W = 213.34 > B_W = 193.97$ then W ≡ (234.01, 234.01, 234.01), but maintaining $R_{min} = R_{BK} = 33.04$, $G_{min} = G_{BK} = 27.08$, $B_{min} = B_{BK} = 27.04$ (r.c.d.e. is different for each spectral channel). Then

$$\beta_{iWW} = \left[1 + \frac{\log(G_i + 1) - \log(234.01 + 1)}{\log(213.34 - 27.08 + 1)}\right] \times 100 \qquad \text{(A3)}$$

- With the without-white condition, if we reject the colorimetric white information, and assume that this absence does not alter the colorimetric encoding of the other stimuli, we have that

under C illuminant, for example, $R_{max} = R_{RP} = 89.24$, $G_{max} = G_B = 100.61$, $B_{max} = B_{PB} = 192.60$, $R_{min} = R_{BK} = 17.58$, $G_{min} = G_{BK} = 18.25$, $B_{min} = B_{BK} = 29.97$. Then

$$\alpha_{i\mathrm{Max}} = \left[1 + \frac{\log(R_i + 1) - \log(89.24 + 1)}{\log(89.24 - 17.58 + 1)}\right] \times 100 \qquad \text{(A4)}$$

In Fig. 7, a high degree of colour constancy is observed in ($\alpha_{i\mathrm{W}}$, $\beta_{i\mathrm{W}}$, $\gamma_{i\mathrm{W}}$) and ($\alpha_{i\mathrm{Max}}$, $\beta_{i\mathrm{Max}}$, $\gamma_{i\mathrm{Max}}$) white encodings/selections because they continue the outlines of Creutzfeldt's relativistic model and photometric rule such as they are implemented in this paper. Because the other white encodings/selections lose colorimetric information about the illuminant, an intermediate degree of colour constancy is shown in ($\alpha_{i\mathrm{E}}$, $\beta_{i\mathrm{E}}$, $\gamma_{i\mathrm{E}}$) and (α_{i}ww, β_{i}ww, γ_{i}ww).